Journal of Materials Chemistry C

Robust Chain Aggregation of Low-Entropy Rigid Ladder Polymer in Solution

Journal:	*Journal of Materials Chemistry C*
Manuscript ID	TC-ART-02-2022-000761.R1
Article Type:	Paper
Date Submitted by the Author:	27-Apr-2022
Complete List of Authors:	Ma, Guorong; University of Southern Mississippi, School of Polymer Science and Engineering Leng, Mingwan; Texas A&M University System, Department of Chemistry Li, Shi; Texas A&M University System, Department of Chemistry Cao, Zhiqiang; University of Southern Mississippi, School of Polymer Science and Engineering Cao, Yirui; Texas A&M University System, Department of Chemistry Tabor, Daniel; Texas A&M University System, Department of Chemistry Fang, Lei; Texas A&M University, Chemistry; Texas A&M University, Materials Science and Engineering Gu, Xiaodan; University of Southern Mississippi, School of Polymer Science and Engineering

Robust Chain Aggregation of Low-Entropy Rigid Ladder Polymer in Solution

Guorong Ma,[a] Mingwan Leng,[b] Shi Li,[b] Zhiqiang Cao,[a] Yirui Cao,[b] Daniel Tabor,[b] Lei Fang,[b*] and Xiaodan Gu[a*]*

[a] School of Polymer Science and Engineering, Center for Optoelectronic Materials and Devices, The University of Southern Mississippi, Hattiesburg, MS, 39406, USA.

[b] Department of Chemistry, Texas A&M University, College Station, TX 77843, USA.

† Electronic supplementary information (ESI) available: Simulation details, UV-Vis, GIWAXS, SANS and AFM results.

Keywords: Conjugated Ladder polymer, backbone flexibility, polymer chain conformation, dynamics light scattering, UV-Vis absorption, neutron scattering, molecular dynamics simulation, entropy change.

Abstract: Conjugated polymers have been widely investigated where the ladder-type conjugated polymers get more attention on account of their rigid backbones and extraordinary properties. However, the understanding of how the rigid conformation of ladder polymers translate to materials properties is still limited. Here we systematically investigated the solution aggregation properties of a carbazole-derived conjugated ladder polymer (**LP**) and its analogous non-ladder control polymer (**CP**) via light scattering, neutron scattering, and UV-Vis absorption spectroscopy characterization techniques, revealing a highly robust, temperature-insensitive aggregation behavior of **LP**. The experimental findings were further validated by computational molecular dynamics simulations. We found that the peak positions and intensities of UV spectra for LP remained constant between 20 ℃ to 120 ℃ in chlorobenzene solution. The polymer also showed stable hydrodynamics radius measured by dynamic light scattering from 20 ℃ to 70 ℃ in chlorobenzene solution. Using small-angle neutron scattering, no Guinier region was reached in the measurement q range down to 0.008 $Å^{-1}$, even at the elevated temperature. In contrast, the non-ladder control polymer **CP** was fully soluble in chlorobenzene solvent without the observation of any notable aggregate. Brownian dynamics simulation showed that during polymer aggregation, the entropy change of **LP** was significantly less negative than that of non-ladder control polymer.

These findings revealed the low entropy nature of rigid conjugated ladder polymers and the low entropy penalty for their aggregation, which is promising for highly robust intermolecular interaction at high temperature. Such unique thermodynamic feature of rigid ladder polymers can be leveraged in the design and application of next-generation electronic and optoelectronic devices that function in unconventional high temperature conditions.

Introduction

Conjugated polymers are prominent materials for various organic electronic and photovoltaic devices due to their soft, deformable, and tunable electronic properties, as well as potential low-cost[1-6]. Conjugated ladder polymers (cLPs), a subtype of conjugated polymers, which feature more than one strand of chemical bond linking the fused conjugated repeat units together, are less energetic disorder and more rigid towards chain bending[7]. cLPs are shown to have superior properties including high intrinsic charge transport[8], low band gap[9, 10], and high stability[11, 12]. Many cLPs have been synthesized with unique electrical and optical properties, including poly(p-phenylene)(LPPP)[13], poly(benzimidazole benzophenanthroline) (BBL)[14], and cLPs derived from perylene-3,4,9,10-tetracarboxylic acid diimides (PDIs)[15], carbazole[16] or fluorene[17] moieties, as well as those bridged by intramolecular coordinate bonds[18, 19]. cLPs are promising materials for a wide range of applications, such as photodetector[20], light emitting diode[21], field-effect transistor[22], thermoelectric device[23], and high performance organic photovoltaic[24-28]. For most of these applications, cLP demonstrated significant higher stability compared to their non-ladder

counterparts thanks to the presence of multiple strands of bonds and the thermodynamically stable fused-ring aromatic backbones.

The chain rigidity of conjugated polymers greatly influences their physical properties and hence electronic performance. With an extra strand of bonds, cLPs are expected to have a stiffer backbone because the additional strand of bonds along the backbone hinders torsional motion in the mainchain[29]. Such enhanced rigidity often leads to lower backbone entropy[30] and stronger interchain interactions. Consequently, cLPs generally exhibit lower solubility compared with non-ladder conjugated polymers due to the lower entropy gain[31] and higher required enthalpy change needed to break the strong inter-chain interactions during the dissolving process. In this context, the solution properties of cLPs, such as chain conformation and solution aggregation, are less explored compared with non-ladder-shaped conjugated polymers.

In the present work, we thoroughly examined the solution properties of a carbazole-derived cLP (**LP**), by comparing with a control polymer **CP** without ladder constitute, through variable-temperature UV-Vis spectroscopy, dynamic light scattering (DLS), small-angle neutron scattering, and molecular dynamics (MD) simulations. The results suggest that, despite being visibly absent of large aggregates in solution, **LP** has a strong thermodynamic tendency to aggregate due to the rigid planar backbone and minimum dissolving entropy change. The small entropy change of the process also leads to remarkable robustness of the resulting aggregate at elevated temperatures. Molecular dynamics simulations on the aggregation process of these two polymers further corroborated the drastically different aggregation entropy values caused by the ladder constituent. This work provides direct physical insights into the role of chain rigidity on solution assembly and aggregation, which is important for solution processing and applications of conjugated polymers.

Experimental section

Materials

Conjugated ladder polymer **LP** and control non-ladder conjugated polymer **CP** were synthesized based on the method as reported previously[16]. The chemical structures of investigated polymers are listed in **Figure 1a**. **LP** was synthesized through two steps, including (i) a step-growth polymerization of two alkene-functionalized monomers to give a polymeric intermediate with preorganized pendant alkene groups, and (ii) subsequently a ring-closing olefin metathesis reaction to form the second thread of $\sigma - \sigma$ bond along the polymer backbone. The molar mass and dispersity ($Đ$) were obtained from a TOSOH EcoSEC (HLC-8320GPC) chromatography at 40 ºC with UV detector at 254 nm and THF as the eluent. The molar masses were calculated using a calibration curve based on the UV absorption signal of polystyrene standards. The solvents chloroform chlorobenzene and o-dichlorobenzene were used as purchased (Sigma Aldrich) without further purification.

Methods

UV-Vis Spectroscopy

UV-Vis spectroscopy was performed on a Cary 5000 UV-Vis-NIR spectrophotometer (Agilent Technologies) with a 10 mm optical path quartz cuvette and customized-built heating elements. A solution is filtered through 0.45 μm PTFE filter (GE healthcare) and heated to the desired temperature before the spectrum is recorded.

Photoluminescence Spectroscopy

Photoluminescence spectroscopy was performed on a PTI-Horiba QuantaMaster 400 Spectrofluorimeter equipped with a 75 W Xe arc lamp in steady-state mode. The solution after filtration was held in a 10mm quartz cuvette at 25±0.5℃ for the measurement.

Dynamic Light Scattering (DLS)

Dynamic light scattering was performed on a Brookhaven BI-200SM research goniometer with BI-APD avalanche photodiode detector and 35mW 633nm laser source with right-angle geometry. Solutions were hold in capped glass tube and the temperature was controlled by an intracooler with cyclic water with a variation of 1℃. An autocorrelation function, C(t) is calculated based on the fluctuation signal:

$$\mathrm{C(t)} = \mathrm{A}e^{-2\Gamma t} + B$$

wherein A is optical constant through instrument design, Γ is relaxation of the fluctuation, t is time and B is the constant background. Γ and q are defined as $\Gamma = Dq^2$ and scattering vector $q = \frac{4\pi\, n_0}{\lambda_0} sin\left(\frac{\theta}{2}\right)$. The size distribution of the particles was analyzed by the Brookhaven software using cumulants analysis.

Small-Angle Neutron Scattering (SANS)

SANS experiments were performed at the extended Q-range small-angle neutron scattering diffractometer (EQ-SANS BL-6) at the Spallation Neutron Source (SNS) located at Oak Ridge National Laboratory (ORNL)[32]. Polymers were dissolved in deuterated chlorobenzene at a concentration of 5 mg□ml^{-1} without further filtration. Solution was held in Hellma quartz cells with a beam path of 2 mm. To cover the range of scattering wavevector q from 0.003 to 0.7 Å^{-1}, two configurations (4m sample to detector distance with a wavelength band of $\lambda_{min} = 12$ Å and 2.5m sample-to-detector distance with $\lambda_{min} =$ 2.5 Å) were used. The experiments were measured at 75 ºC. Scattering intensity was reduced by subtracting the background from solvents and cells and put on an absolute scale (cm^{-1}) by using a standard porous silica sample[33]. Scattering signal was analyzed using SasView software and fitted with suitable models as described later.

Atomic Force Microscopy (AFM)

Thin film was spin coated onto clean silicon wafer from chloroform solution. AFM images of spin coated LP and CP films were acquired on an Asylum Research Cypher S instrument operating in tapping mode in air.

Grazing-Incidence Wide-Angle X-ray Scattering (GI-WAXS)

GIWAXS of polymeric thin films on silicon substrate were performed on a laboratory beamline system (Xenocs Inc. Xeuss 2.0) with an X-ray wavelength of 1.54 Å and sample to detector distance of 15 cm. An incidence angle of 0.2° was used. Samples were kept under vacuum to minimize air scattering. Diffraction images were recorded on a Pilatus 1M detector (Dectris Inc.) with an exposure time of 1.5 h and processed using the Nika software package, in combination with WAXSTools using Wavemetrics Igor.

Molecular Dynamics Simulations

The simulation of the aggregation of the **CP** and **LP** polymers is challenging due to the number of potential degrees of freedom in the system and the importance of solvent effects. Two types of simulations were implemented in tandem to efficiently explore the conformational landscape without sacrificing a robust treatment of the aggregation thermodynamics. The chains were simulated first with Brownian dynamics (BD) simulation with an implicit solvent. Here, frictional and random forces are added to a conventional molecular dynamics of the polymer, allowing for an accounting of the dynamic effects of the solvent at lower computational cost. This allows for the initial simulations to access much longer simulated timescales than could be accessed with atomistic solvent simulations.

The simulation workflow is shown in **Figure S1**. First, a single polymer chain of **CP** (with 16 repeat units) or **LP** (8 repeat units) was placed in the center of a cubic box (side length 20 nm) with implicit solvent and equilibrated for 5 ns using Brownian dynamics simulation. Then, 10 of

the equilibrated polymer chains were inserted into new $20 \times 20 \times 20$ nm cubic boxes to make the concentrated CP or LP polymer systems. Each system was further equilibrated with implicit solvent under the same condition for another 10 ns. The initial and final configurations of these implicit solvent simulations were then explicitly solvated with a pre-equilibrated 1,2-dichlorobenzene solvent. Then, all-atomic MD simulations were carried out to each of these systems using a leap-frog integrator with 2 fs time step. The entropies of the systems were calculated with the two-phase thermodynamics (2PT) model[34, 35] using the DoSPT code developed by Caro and co-workers[36, 37]. All simulations were carried out at 384 K and repeated eight times for statistics. Further details of the simulation process can be found in the supporting information.

Results and Discussion

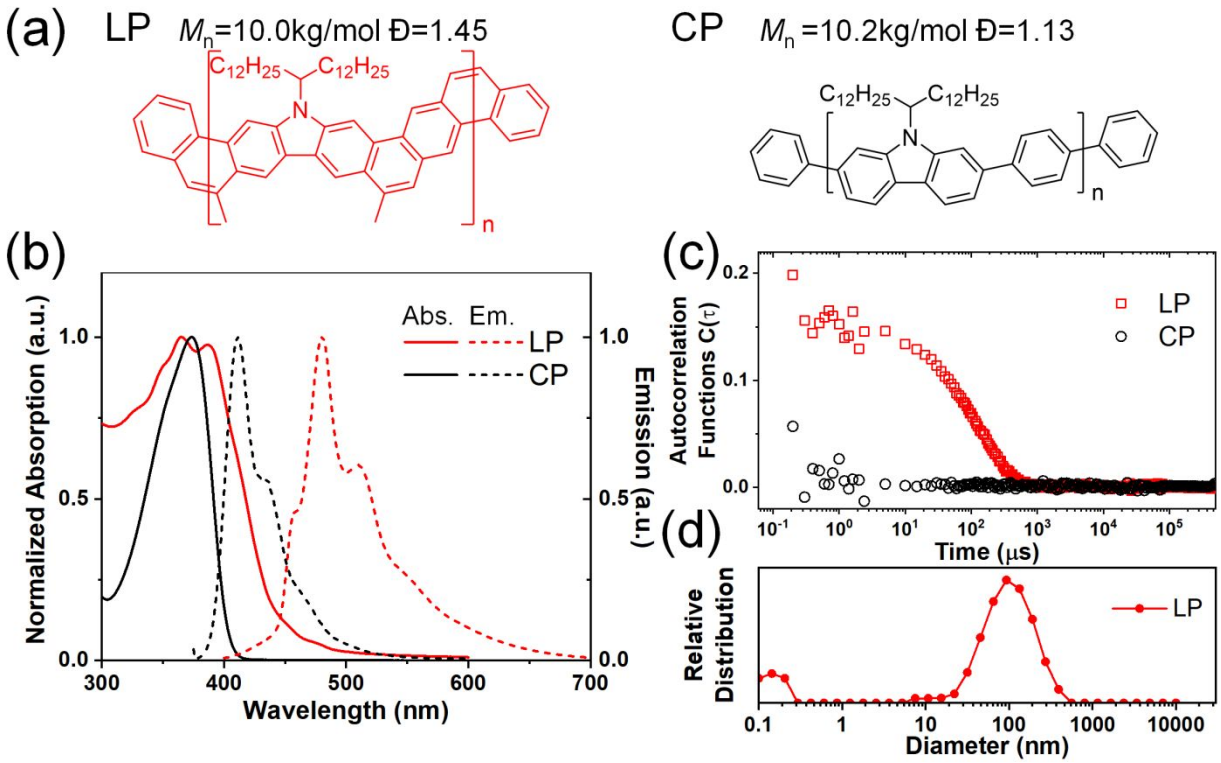

Figure 1 (a) Structural formulas of LP and CP used in this work. The molar mass and distribution are labeled. (b) UV-Vis absorption (solid lines) and photoluminescence spectroscopy (dashed lines) of LP and CP in chloroform (~0.05 mg/ml) at 20 °C. (c) Autocorrelation functions of LP and CP. (d) Size distribution of LP by intensity in the solution as a function of particle diameter. (a) Structural formulas of **LP** and **CP** used in this work. The molecular weight and distribution are labeled. (b) Normalized UV-Vis absorption (solid lines) and photoluminescence spectra (dashed lines) of **LP** and **CP** in chloroform (~0.05 mg/ml) at 20 ^{o} C. (c) Autocorrelation functions of **LP** and **CP** in chloroform solvent. (d) Size distribution of **LP** aggregates by intensity in the solution as a function of particle diameter.

Carbazole-derived polymer **LP** (**Figure 1a**) is selected as a representative model for cLP because (i) it has a very low level of defects along the ladder-type backbone on account of the highly efficient thermodynamic annulation method (ring-closing olefin metathesis) for its synthesis[16]; and (ii) it possesses good apparent dispersibility in solution despite the ladder-type constitution. We aim to compare the solution assembly of **LP** with its non-ladder polymer counterpart **CP (Figure 1a)**. Both **LP** and **CP** were synthesized in fresh batches with similar molecular weight in this study. They can be both dissolved/dispersed in common organic solvents and give apparently clear solutions. The solutions of **LP** and **CP** can both pass through 0.45 μm filter membranes and give clear UV/vis absorption and fluorescent emission spectra (**Figure 1b**). Our previous study[38] on the optical properties of **LP** suggested the formation of H-aggregate in solution. The lowest energy absorption band of LP (~450 nm)[16, 38] is extremely weak and can be easily ignored. Considering this absorption peak and the lowest energy emission peak at 456 nm (Figure S2), LP exhibits an extremely small Stokes shift as expected for a highly rigid conjugated ladder polymer. Here dynamic light scattering (DLS) was used to probe the solution aggregation of **LP** and **CP** (**Figure 1c**). It is noteworthy that neither **LP** nor **CP** absorbs the wavelength of laser used in the DLS study (633 nm) so that no absorptive interference is encountered during the measurement. The

aggregation formation of **LP** was confirmed by DLS, which showed a single decay in the autocorrelation function, corresponding to aggregation with an average hydrodynamic radius of 100 nm. The **CP** solution, in contrast, gave a flat signal, indicating that **CP** is fully dissolved in chloroform.

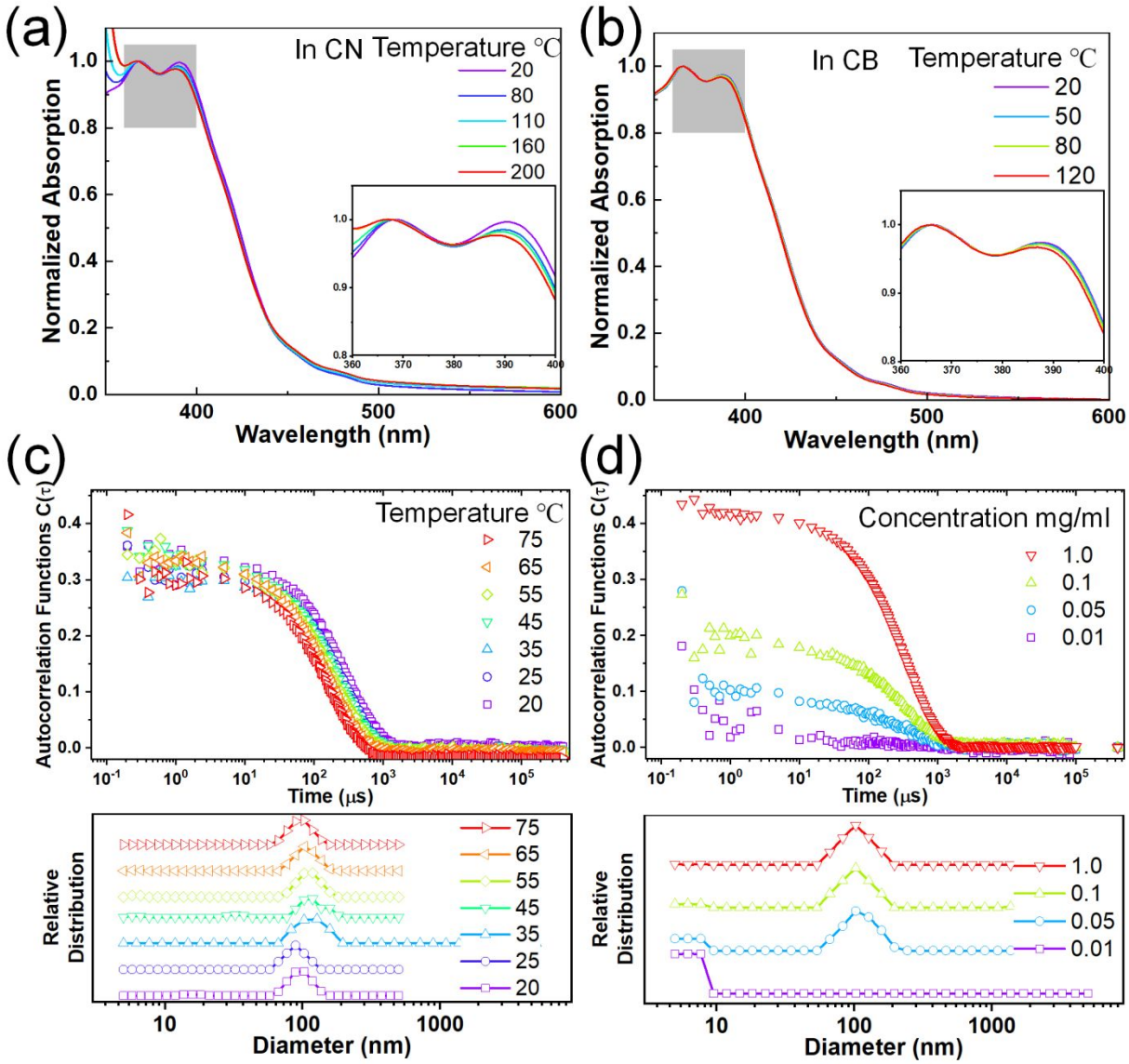

Figure 2. Variable temperature UV-Vis spectra of **LP** in (a) chloronaphthalene (CN) and (b) chlorobenzene (CB) normalized by 0-1 peak. The inset shows a magnified view of the gray area. Temperature-dependent (c) and concentration-dependent (d) DLS result of **LP** in chlorobenzene and the correspond size distribution.

To test the potential dissociation of these aggregates in variable conditions, we performed UV-Vis spectroscopy for **LP** dispersed in several different solvents at varied temperatures. 1-chloronaphelene (CN) and chlorobenzene (CB) were selected as the solvents because they are known to be highly efficient in breaking pi-pi aggregates and can be heated to high temperatures thanks to their high boiling points.[39] As shown in **Figure 2 (a)** and **(b)**, when dispersed in these solvents, **LP** showed similar absorption profiles with that in chloroform. Remarkably, at higher temperatures (up to 200 ˚C for CN and 120 ˚C for CB), the solution spectra of **LP** maintained almost the same with only marginal change of the ratio of 0-0 / 0-1 peaks, despite the fact that **LP** is aggregated in solution. In contrast, for **CP** solution in CB, the absorption peaks showed a red shift from 378 nm at 20℃ to 375 nm at 120℃ (**Error! Reference source not found.3**) due to conformational change of the fully dissolved chains. Variable UV-vis spectra of **LP** were also recorded in other solvents such as chloroform, and dichlorobenzene, all showing similar peak profiles with marginal changes upon heating as shown in **Figure S4**. This observation indicates that **LP** chains maintained its aggregation form, and there is no significant conformational change on the ladder type backbone at elevated temperatures as high as 200 ˚C. Notably, this weak temperature dependence of absorption is also observed independently in other conjugated ladder

polymers[31]. This behavior is typically not observed on conventional, non-ladder type conjugated polymer[40-42]. The stable aggregation of **LP** at high temperatures was also confirmed by DLS as the hydrodynamic radius remained constant at elevated temperatures up to the limit of our instrument (75 ˚C) (**Figure 2c)**. Variable concentration DLS measurements were also conducted on **LP** (**Figure 2d**), as it is known that decreasing concentration can break the **LP** aggregation[38]. These DLS data show that **LP** remained aggregated at concentrations as low as 0.05 mg/ml in CB solution and 0.005 mg/ml in chloroform solution (**Figure S5**). We also tested the DLS of a low molecular weight batch of oligomeric **LP** (M_n ~ 3 kg/mol), showing a peak hydrodynamic radius of 30 nm (**Figure S6**), suggesting significant aggregation even for this low molecular weight batch. Our finding indicates that the aggregation of **LP** in various solutions is highly robust and insensitive to solution temperature.

To further characterize the aggregation of **LP**, we conducted small-angle neutron scattering (SANS) on both **LP** and **CP** solutions dissolved in deuterated chlorobenzene at 75℃. As shown in **Figure 3(c)**, the scattering profile for **LP** never reach its Guinier region in the measurement range (0.008 Å $^{-1}$ < Q < 0.3 Å $^{-1}$), as indicated by scattering intensity continue to raise as at the low q region, following the trend of $I \propto q^{-1.76}$. These data suggested that **LP** solution forms large

aggregation in the experimental condition. In contrast, the scattering profile for **CP** reached Guinier region as evidenced from a plateau at lower q, suggesting well-dispersed polymer chains in solution. Hence, we used two different fitting models to fit the curves, namely, parallelepiped model[43] for **LP** and flexible cylinder model[44] for **CP**. The fitting parameters are shown in **Figure 3**. **LP** can be modeled by elongated parallelepiped with a large dimension c = 1978.8 Å, which was much larger than single-chain contour length (around 17.9 nm, see **Figure S7**) so it must be an aggregated package of multiple chains. **CP** has a contour length (L_c) of 122.7 Å and a small cylinder diameter (R) of 8.9 Å, which is reasonable for a dissolved non-ladder single chain with the molar mass around 10 kg/mol. Temperature-dependent SANS on **LP** also showed the presence of large aggregates at 25℃ and 50℃ (**Figure S8** and **Error! Reference source not found.**), which was in accordance with the UV-Vis and DLS results. These data demonstrate the size and robustness of **LP** aggregates in solution. It is also noteworthy that the single-chain conformation of **LP** cannot be directly probed by SANS due to its strong aggregation in the wide temperature range we have measured.

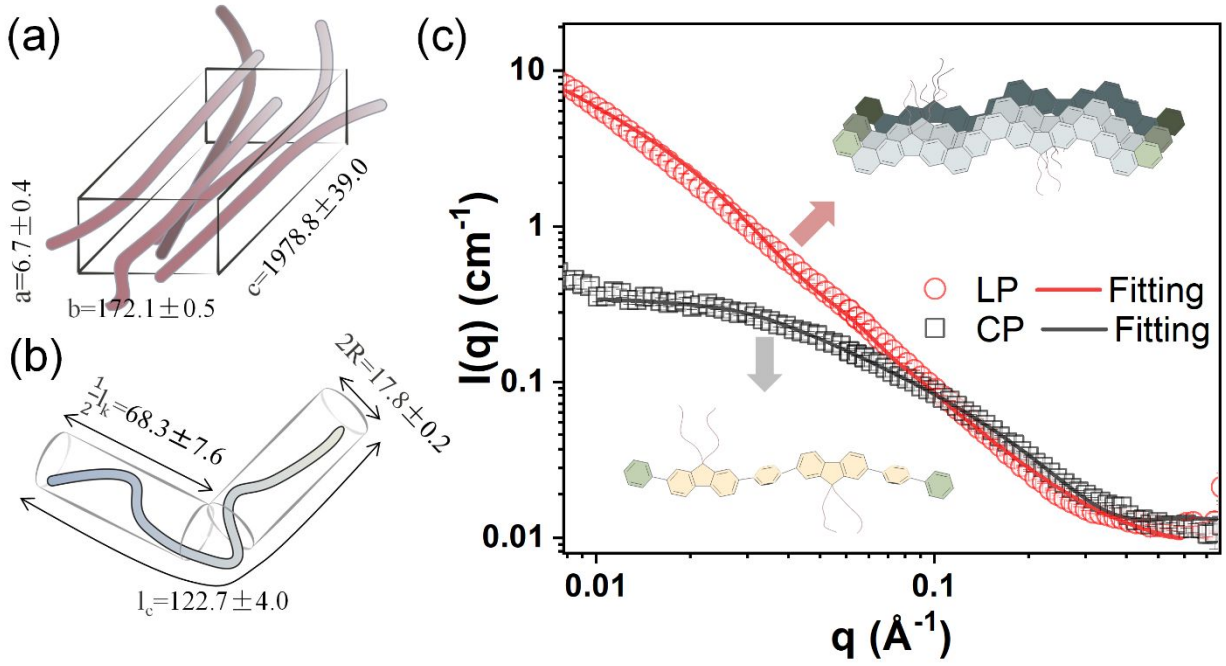

Figure 3. Chain model and fitting results for SANS analysis (length unit in Å). (a) parallelepiped model for **LP** and (b) flexible cylinder model for **CP**. (c) SANS data and fitting curve. Insert illustrate the chain conformation of the **LP** (top) and **CP** (bottom)

To elucidate the chain packing mode in the **LP** aggregates, we conducted the atomic force microscopy (AFM) and grazing incidence wide-angle X-ray scattering (GI-WAXS) on the **LP** thin film. Because the **LP** aggregates are stable towards heat and solvents, the morphology for chain aggregate is expected to be maintained from solution to the solid-state through spin coating process. On the samples spun coated from a dilute solution (**Figure S9**), we only observed round particles on the wafer rather than large thin sheets seen on other conjugated polymers assembled

by strong $\pi - \pi$ stacking[45, 46]. Thicker **LP** film (40 nm) was prepared by drop cast chloroform solution onto Silicon wafer, and GI-WAXS result only showed a broad isotropic scattering peak without a strong scattering profile (**Figure S10**), indicating an amorphous nature of the **LP** aggregates. This observation does not contradict the rigid chain feature, as similar behavior has been observed in many rigid rod polymers[47]. This amorphous feature was also reported in other fully conjugated ladder polymers[16, 48], although thermal annealing on solid films can improve the crystallinity for certain ladder polymers[49] and rigid conjugated polymers[50, 51]. The absence of crystallinity in fully conjugated ladder polymers can be attributed to (i) the strong dynamic aggregation already formed in solution, and (ii) the lack of chain mobility of the large and rigid polymer backbone during the transition from solution to the solid state, as demonstrated in our previous systematic study on a series of ladder-type oligomers[52]. This lack of crystalline domain and the presence of long alkyl side-chain prevents fast charge transport in the solid state of LP as mentioned previously.[16]

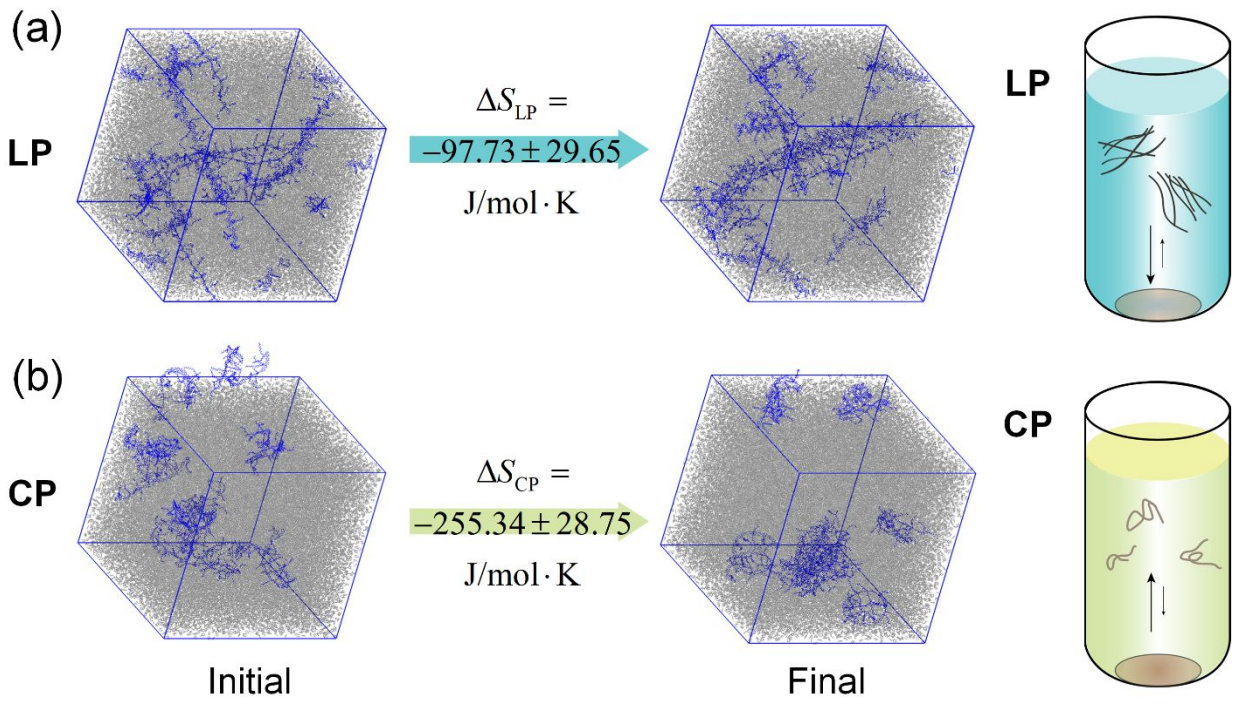

Figure 4. Snapshots of the initial and finial chain conformations of **LP** (a) and **CP** (b) from a single simulation. The polymer chains are colored in blue and the atomic solvents are colored in gray. The entropy changes associated with the aggregation processes were shown above. An illustration of the dissolving process of **LP** and **CP** is shown next to it.

We hypothesized that the lack of temperature dependence of **LP** aggregation was a result of small entropy change during the process. It is envisioned and demonstrated that a ladder type polymer chain possesses a much lower initial entropy compared to conventional polymers with free torsional motions about the main chain. Thereby, the aggregation of such rigid ladder-type

chains would induce minimal restriction on the degree of freedom of the chain, and hence impose a much smaller entropy cost for aggregation. To test this hypothesis, the molecular simulations were performed to elucidate the entropy change during the aggregation process in *o*-dichlorobenzene. The results of one of the eight simulations are shown in **Figure 4**, illustrating the chain conformation before and after energy optimization. As expected, the **LP** is straighter after the energy optimization, but it contains a select number of twists and bends that persist much longer time to be flattened, in agreement with reports on another ladder polymer[53]. The entropy change of this process is calculated using the formula:

$$\Delta S_{LP} = S_{dissolved\ LP} - S_{solid\ LP} \text{ and } \Delta S_{CP} = S_{dissolved\ CP} - S_{solid\ CP},$$

Where the $S_{dissolved}$ and S_{solid} are the total entropt of the polymer system at initial and final states, respectively. The difference of these states represents the reverse of dissolving process. The calculated entropy values from eight individual simulations were listed in **Error! Reference source not found.** and the cluster analysis to monitor the aggregation process from the BD simulations were plotted in **Error! Reference source not found.11**. At the end of the simulation procedures, the **LP** has fewer aggregated clusters and larger cluster sizes compared to the **CP**. Although both ΔS_{LP} and ΔS_{CP} are negative for these process, indicating entropy lost during aggregation, the ΔS_{LP} value (-97.73 ± 29.65 J•mol^{-1}•K^{-1}) was significantly smaller in absolute value compared with ΔS_{CP} (-255.34 ± 28.75 J•mol^{-1}•K^{-1}), representing a significantly less entropy cost for **LP** to aggregate, and hence much smaller temperature-dependent process for its

dissolution and aggregation. These computational results also indicate that much bulky side chain is necessary to fully dissolve rigid ladder polymers by compensation the low entropy gain during dissolution[22].

We expect the low temperature dependence of aggregation can be ubiquitous among other rigid ladder polymers. This feature should be considered and perhaps exploited as a critical feature during the solution processing of ladder polymers for sold state applications. for example. if a polymer aggregation feature in solution needs to be maintained in the solid state through solution processing and thermal annealing, a rigid ladder-type backbone can be designed to give the desired robustness for the aggregation, which is insensitive to thermal annealing and solvent attack.

Conclusions

To conclude, we characterized solution aggregation properties of a low-defect ladder conjugated polymer **LP** and its non-ladder conjugated polymer control **CP**, through temperature-dependent UV-Vis, DLS, and small-angle neutron scattering investigations, combined with molecular dynamics simulation. We elucidated that **LP** forms stable aggregates in solution and maintains aggregated at elevated temperatures up to 200 ˚C. We also demonstrated the amorphous nature of the aggregation in solution and in the thin film state for GIWAXS measurement. Brownian dynamics simulation showed that **LP** had a low entropy decrease during the chain aggregation process caused by the low-entropy rigid ladder-type backbone. These results highlight the role of chain conformation in the thermodynamic properties of rigid ladder polymers in solution and in

the solid state. The small temperature dependence of ladder polymer aggregation should be considered and exploited during the solution processing of these materials for solid state applications.

Supporting Information

The Supporting Information is available free of charge.

Corresponding Author

*(X.G.) Email: xiaodan.gu@usm.edu; (L.F.) Email: fang@chem.tamu.edu; (D.T.) Email: daniel.tabor@tamu.edu

Author Contributions

Guorong Ma performed the characterization of LP and CP using UV-Vis/PL/DLS/AFM/GIWAXS. Mingwan Leng and Yirui Cao synthesized and purified LP and CP and characterized by NMR/GPC. Zhiqiang Cao performed the SANS experiments and analyzed the data. Li Shi and Daniel Tabor designed, conducted, and analyzed the MD simulations. The manuscript was written by Guorong Ma and Mingwan Leng. All authors have given approval to the final version of the manuscript. Xiaodan Gu and Lei Fang conceived the idea, coordinated, and supervised the research project.

Conflicts of interest

The authors declare no competing financial interest.

Acknowledgments

This work is financially supported by the U.S. National Science Foundation (NSF) under award number of No. CHE 2004133 and 2003733. We thank the Center for Nanophase Materials Sciences under the support of DOE for the SANS characterization. This work benefited from the use of the SasView application, originally developed under NSF Award DMR-0520547. SasView contains code developed with funding from the European Union's horizon 2020 research and innovation programme under the SINE20. D.P.T. and S.L acknowledge support from Texas A&M University Startup Funding. Portions of this research were conducted with high-performance research computing resources provided by Texas A&M University HPRC. D.P.T. acknowledges the Texas A&M Institute of Data Science Career Initiation Fellowship.

Notes and references

1. Sirringhaus, H., 25th Anniversary Article: Organic Field-Effect Transistors: The Path Beyond Amorphous Silicon. *Adv. Mater.* 2014, *26* (9), 1319-1335.

2. Bao, Z.; Chen, X., Flexible and Stretchable Devices. *Adv. Mater.* 2016, *28* (22), 4177-4179.

3. Onorato, J.; Pakhnyuk, V.; Luscombe, C. K., Structure and design of polymers for durable, stretchable organic electronics. *Polym. J.* **2016,** *49* (1), 41-60.

4. Gu, X.; Zhou, Y.; Gu, K.; Kurosawa, T.; Guo, Y.; Li, Y.; Lin, H.; Schroeder, B. C.; Yan, H.; Molina-Lopez, F.; Tassone, C. J.; Wang, C.; Mannsfeld, S. C. B.; Yan, H.; Zhao, D.; Toney, M. F.; Bao, Z., Roll-to-Roll Printed Large-Area All-Polymer Solar Cells with 5% Efficiency Based on a Low Crystallinity Conjugated Polymer Blend. *Adv. Energy Mater.* **2017,** *7* (14), 1602742.

5. Xu, J.; Wu, H. C.; Zhu, C.; Ehrlich, A.; Shaw, L.; Nikolka, M.; Wang, S.; Molina-Lopez, F.; Gu, X.; Luo, S.; Zhou, D.; Kim, Y. H.; Wang, G. N.; Gu, K.; Feig, V. R.; Chen, S.; Kim, Y.; Katsumata, T.; Zheng, Y. Q.; Yan, H.; Chung, J. W.; Lopez, J.; Murmann, B.; Bao, Z., Multi-scale ordering in highly stretchable polymer semiconducting films. *Nat. Mater.* **2019,** *18* (6), 594-601.

6. Wang, J.; Zhao, C.; Zhou, L.; Liang, X.; Li, Y.; Sheng, G.; Du, Z.; Tang, J., An Effective Strategy to Design a Large Bandgap Conjugated Polymer by Tuning the Molecular Backbone Curvature. *Macromol. Rapid Commun.* **2021,** *42* (10), 2000757.

7. Lee, J.; Kalin, A. J.; Yuan, T.; Al-Hashimi, M.; Fang, L., Fully conjugated ladder polymers. *Chem. Sci.* **2017,** *8* (4), 2503-2521.

8. Prins, P.; Grozema, F. C.; Schins, J. M.; Patil, S.; Scherf, U.; Siebbeles, L. D., High intrachain hole mobility on molecular wires of ladder-type poly(p-phenylenes). *Phys. Rev. Lett.* **2006,** *96* (14), 146601.

9. Kertesz, M.; Hughbanks, T. R., Low bandgap ladder polymers. *Synth. Met.* **1995,** *69* (1-3), 699-700.

10. Tsuda, A.; Osuka, A., Fully conjugated porphyrin tapes with electronic absorption bands that reach into infrared. *Science* **2001,** *293* (5527), 79-82.

11. Wang, S.; Hong, W.; Ren, S.; Li, J.; Wang, M.; Gao, X.; Li, H., New ladder-type conjugated polymer with broad absorption, high thermal stability, and low band gap. *J. Polym. Sci., Part A: Polym. Chem.* **2012,** *50* (20), 4272-4276.

12. Zou, Y.; Ji, X.; Cai, J.; Yuan, T.; Stanton, D. J.; Lin, Y.-H.; Naraghi, M.; Fang, L., Synthesis and Solution Processing of a Hydrogen-Bonded Ladder Polymer. *Chem* **2017,** *2* (1), 139-152.

13. Scherf, U.; Müllen, K., A soluble ladder polymer via bridging of functionalized poly(p-phenylene)-precursors. *Die Makromolekulare Chemie, Rapid Communications* **1991,** *12* (8), 489-497.

14. Jenekhe, S. A.; Johnson, P. O., Complexation-mediated solubilization and processing of rigid-chain and ladder polymers in aprotic organic solvents. *Macromolecules* **1990,** *23* (20), 4419-4429.

15. Huang, C.; Barlow, S.; Marder, S. R., Perylene-3,4,9,10-tetracarboxylic acid diimides: synthesis, physical properties, and use in organic electronics. *J. Org. Chem.* **2011,** *76* (8), 2386-2407.

16. Lee, J.; Rajeeva, B. B.; Yuan, T.; Guo, Z. H.; Lin, Y. H.; Al-Hashimi, M.; Zheng, Y.; Fang, L., Thermodynamic synthesis of solution processable ladder polymers. *Chem. Sci.* **2016,** *7* (2), 881-889.

17. Trilling, F.; Ausländer, M.-K.; Scherf, U., Ladder-Type Polymers and Ladder-Type Polyelectrolytes with On-Chain Dibenz[a,h]anthracene Chromophores. *Macromolecules* **2019,** *52* (8), 3115-3122.

18. Grandl, M.; Schepper, J.; Maity, S.; Peukert, A.; von Hauff, E.; Pammer, F., N → B Ladder Polymers Prepared by Postfunctionalization: Tuning of Electron Affinity and Evaluation as Acceptors in All-Polymer Solar Cells. *Macromolecules* **2019,** *52* (3), 1013-1024.

19. Cao, Y.; Zhu, C.; Barlog, M.; Barker, K. P.; Ji, X.; Kalin, A. J.; Al-Hashimi, M.; Fang, L., Electron-Deficient Polycyclic pi-System Fused with Multiple B<--N Coordinate Bonds. *J. Org. Chem.* **2021,** *86* (3), 2100-2106.

20. Wang, Q.; Qi, J.; Qiao, W.; Wang, Z. Y., Soluble ladder conjugated polypyrrones: Synthesis, characterization and application in photodetectors. *Dyes Pigm.* **2015,** *113*, 160-164.

21. Qiu, S.; Lu, P.; Liu, X.; Shen, F.; Liu, L.; Ma, Y.; Shen, J., New Ladder-Type Poly(p-phenylene)s Containing Fluorene Unit Exhibiting High Efficient Electroluminescence. *Macromolecules* **2003,** *36* (26), 9823-9829.

22. Kim, F. S.; Park, C. H.; Na, Y.; Jenekhe, S. A., Effects of ladder structure on the electronic properties and field-effect transistor performance of Poly(benzobisimidazobenzophenanthroline). *Org. Electron.* **2019,** *69*, 301-307.

23. Wang, S.; Sun, H.; Ail, U.; Vagin, M.; Persson, P. O.; Andreasen, J. W.; Thiel, W.; Berggren, M.; Crispin, X.; Fazzi, D.; Fabiano, S., Thermoelectric Properties of Solution-

Processed n-Doped Ladder-Type Conducting Polymers. *Adv. Mater.* **2016,** *28* (48), 10764-10771.

24. Xu, Y. X.; Chueh, C. C.; Yip, H. L.; Ding, F. Z.; Li, Y. X.; Li, C. Z.; Li, X.; Chen, W. C.; Jen, A. K., Improved charge transport and absorption coefficient in indacenodithieno[3,2-b]thiophene-based ladder-type polymer leading to highly efficient polymer solar cells. *Adv. Mater.* **2012,** *24* (47), 6356-6361.

25. Sakthivel, P.; Song, H. S.; Chakravarthi, N.; Lee, J. W.; Gal, Y.-S.; Hwang, S.; Jin, S.-H., Synthesis and characterization of new indeno[1,2-b]indole-co-benzothiadiazole-based π-conjugated ladder type polymers for bulk heterojunction polymer solar cells. *Polymer* **2013,** *54* (18), 4883-4893.

26. Chen, Y. L.; Kao, W. S.; Tsai, C. E.; Lai, Y. Y.; Cheng, Y. J.; Hsu, C. S., A new ladder-type benzodi(cyclopentadithiophene)-based donor-acceptor polymer and a modified hole-collecting PEDOT:PSS layer to achieve tandem solar cells with an open-circuit voltage of 1.62 V. *Chem. Commun.* **2013,** *49* (70), 7702-7704.

27. Lee, M.; Hahn, S.-J.; Kim, T.-H., A Phenylene-alkylated Thiophene-based Partially Ladder-type Conjugated Polymer. *Bull. Korean Chem. Soc.* **2013,** *34* (8), 2495-2498.

28. Shao, X.; Dou, C.; Liu, J.; Wang, L., A new building block with intramolecular D-A character for conjugated polymers: ladder structure based on B←N unit. *Science China Chemistry* **2019,** *62* (10), 1387-1392.

29. Petekidis, G.; Fytas, G.; Scherf, U.; Mllen, K.; Fleischer, G., Dynamics of poly(p-phenylene) ladder polymers in solution. *J. Polym. Sci., Part B: Polym. Phys.* **1999,** *37* (16), 2211-2220.

30. Che, S.; Pang, J.; Kalin, A. J.; Wang, C.; Ji, X.; Lee, J.; Cole, D.; Li, J.-L.; Tu, X.; Zhang, Q.; Zhou, H.-C.; Fang, L., Rigid Ladder-Type Porous Polymer Networks for Entropically Favorable Gas Adsorption. *ACS Mater. Lett.* **2019,** *2* (1), 49-54.

31. Huang, Y.-W.; Lin, Y.-C.; Li, J.-S.; Chen, W.-C.; Chueh, C.-C., Investigating the backbone conformation and configuration effects for donor–acceptor conjugated polymers with ladder-type structures synthesized through Aldol polycondensation. *J. Mater. Chem. C* **2021,** *9* (30), 9473-9483.

32. Zhao, J. K.; Gao, C. Y.; Liu, D., The extended Q-range small-angle neutron scattering diffractometer at the SNS. *J. Appl. Crystallogr.* **2010,** *43* (5), 1068-1077.

33. Heller, W. T.; Cuneo, M.; Debeer-Schmitt, L.; Do, C.; He, L.; Heroux, L.; Littrell, K.; Pingali, S. V.; Qian, S.; Stanley, C., The suite of small-angle neutron scattering instruments at Oak Ridge National Laboratory. *J. Appl. Crystallogr.* **2018,** *51* (2), 242-248.

34. Lin, S.-T.; Blanco, M.; Goddard, W. A., The two-phase model for calculating thermodynamic properties of liquids from molecular dynamics: Validation for the phase diagram of Lennard-Jones fluids. *The Journal of Chemical Physics* **2003,** *119* (22), 11792-11805.

35. Lin, S. T.; Maiti, P. K.; Goddard, W. A., 3rd, Two-phase thermodynamic model for efficient and accurate absolute entropy of water from molecular dynamics simulations. *J. Phys. Chem. B* **2010,** *114* (24), 8191-8.

36. Caro, M. A.; Laurila, T.; Lopez-Acevedo, O., Accurate schemes for calculation of thermodynamic properties of liquid mixtures from molecular dynamics simulations. *The Journal of Chemical Physics* **2016,** *145* (24), 244504.

37. Caro, M. A.; Lopez-Acevedo, O.; Laurila, T., Redox Potentials from Ab Initio Molecular Dynamics and Explicit Entropy Calculations: Application to Transition Metals in Aqueous Solution. *J. Chem. Theory Comput.* **2017,** *13* (8), 3432-3441.

38. Hollingsworth, W. R.; Lee, J.; Fang, L.; Ayzner, A. L., Exciton Relaxation in Highly Rigid Conjugated Polymers: Correlating Radiative Dynamics with Structural Heterogeneity and Wavefunction Delocalization. *ACS Energy Lett.* **2017,** *2* (9), 2096-2102.

39. Zhao, K. F.; Zhang, Q.; Chen, L.; Zhang, T.; Han, Y. C., Nucleation and Growth of P(NDI2OD-T2) Nanowires via Side Chain Ordering and Backbone Planarization. *Macromolecules* **2021,** *54* (5), 2143-2154.

40. Ma, W.; Yang, G.; Jiang, K.; Carpenter, J. H.; Wu, Y.; Meng, X.; McAfee, T.; Zhao, J.; Zhu, C.; Wang, C.; Ade, H.; Yan, H., Influence of Processing Parameters and Molecular Weight on the Morphology and Properties of High-Performance PffBT4T-2OD:PC71BM Organic Solar Cells. *Adv. Energy Mater.* **2015,** *5* (23).

41. Heintges, G. H. L.; Leenaers, P. J.; Janssen, R. A. J., The effect of side-chain substitution and hot processing on diketopyrrolopyrrole-based polymers for organic solar cells. *J. Mater. Chem. A* **2017,** *5* (26), 13748-13756.

42. Heuvel, R.; Colberts, F. J. M.; Li, J.; Wienk, M. M.; Janssen, R. A. J., The effect of side-chain substitution on the aggregation and photovoltaic performance of diketopyrrolopyrrole-alt-dicarboxylic ester bithiophene polymers. *J. Mater. Chem. A* **2018,** *6* (42), 20904-20915.

43. Keum, J. K.; Xiao, K.; Ivanov, I. N.; Hong, K.; Browning, J. F.; Smith, G. S.; Shao, M.; Littrell, K. C.; Rondinone, A. J.; Andrew Payzant, E.; Chen, J.; Hensley, D. K., Solvent quality-induced nucleation and growth of parallelepiped nanorods in dilute poly(3-hexylthiophene) (P3HT) solution and the impact on the crystalline morphology of solution-cast thin film. *CrystEngComm* **2013,** *15* (6), 1114-1124.

44. Pedersen, J. S.; Schurtenberger, P., Scattering Functions of Semiflexible Polymers with and without Excluded Volume Effects. *Macromolecules* **1996,** *29* (23), 7602-7612.

45. Zhu, J.; Han, Y.; Kumar, R.; He, Y.; Hong, K.; Bonnesen, P. V.; Sumpter, B. G.; Smith, S. C.; Smith, G. S.; Ivanov, I. N.; Do, C., Controlling molecular ordering in solution-state conjugated polymers. *Nanoscale* **2015,** *7* (37), 15134-41.

46. Yao, Z. F.; Wang, Z. Y.; Wu, H. T.; Lu, Y.; Li, Q. Y.; Zou, L.; Wang, J. Y.; Pei, J., Ordered Solid-State Microstructures of Conjugated Polymers Arising from Solution-State Aggregation. *Angew. Chem. Int. Ed.* **2020,** *59* (40), 17467-17471.

47. Gaudiana, R. A.; Minns, R. A.; Sinta, R.; Weeks, N.; Rogers, H. G., Amorphous rigid-rod polymers. *Prog. Polym. Sci.* **1989,** *14* (1), 47-89.

48. Bheemireddy, S. R.; Hautzinger, M. P.; Li, T.; Lee, B.; Plunkett, K. N., Conjugated Ladder Polymers by a Cyclopentannulation Polymerization. *J. Am. Chem. Soc.* **2017,** *139* (16), 5801-5807.

49. Wang, S.; Ruoko, T. P.; Wang, G.; Riera-Galindo, S.; Hultmark, S.; Puttisong, Y.; Moro, F.; Yan, H.; Chen, W. M.; Berggren, M.; Muller, C.; Fabiano, S., Sequential Doping of Ladder-Type Conjugated Polymers for Thermally Stable n-Type Organic Conductors. *ACS Appl. Mater. Interfaces* **2020,** *12* (47), 53003-53011.

50. Yuan, D.; Awais, M. A.; Sharapov, V.; Liu, X.; Neshchadin, A.; Chen, W.; Bera, M.; Yu, L., Foldable semi-ladder polymers: novel aggregation behavior and high-performance solution-processed organic light-emitting transistors. *Chem. Sci.* **2020,** *11* (41), 11315-11321.

51. Lu, Y.; Wang, J. Y.; Pei, J., Achieving Efficient n-Doping of Conjugated Polymers by Molecular Dopants. *Acc. Chem. Res.* **2021,** *54* (13), 2871-2883.

52. Lee, J.; Li, H.; Kalin, A. J.; Yuan, T.; Wang, C.; Olson, T.; Li, H.; Fang, L., Extended Ladder-Type Benzo[k]tetraphene-Derived Oligomers. *Angew. Chem. Int. Ed.* **2017,** *56* (44), 13727-13731.

53. Unruh, M. T.; Scherf, U.; Bahmann, H.; Rodrigues, A. C. B.; Cunha, C.; Seixas de Melo, J. S.; Schedlbauer, J.; Lupton, J. M., Unexpectedly flexible graphene nanoribbons with a polyacene ladder skeleton. *J. Mater. Chem. C* **2021**, *9* (45), 16208-16216.